Electronic Supplementary Material (ESI) for ChemComm.

Chemical controls on uranyl citrate speciation and the self-assembly of nanoscale macrocycles in aqueous solutions.

M. Basile, D. K. Unruh, K. Gojdas, E. Flores, L. Streicher, and T.Z. Forbes

Synthesis. Uranyl nitrate hexahydrate (Flinn Scientific Inc.), citric acid monohydrate (J.T. Baker), piperazine hexahydrate (Alfa Aesar), ethylenediamine (Sigma Aldrich), pyridine (Fisher Scientific), sodium hydroxide (Fisher Scientific), potassium chloride (Sigma Aldrich) and magnesium nitrate (Sigma Aldrich) were reagent grade and used without further purification. Millipore-filtered ultrapure water (18.2 MΩ resistance) was provided by a ThermoScientific Barnstead EasyPure II which was used in all of the syntheses.

$[C_4H_{12}N_2][(UO_2)_2(C_6H_5O_7)_2](H_2O)_6$: U2-pip was synthesized with a 1:4 molar ratio of 0.2 M $UO_2(NO_3)_2{\cdot}6H_2O$ to 0.2 M $C_6H_8O_7{\cdot}H_2O$. The pH of a citric acid (4 mL 0.2 M, 0.8 mmol) and uranyl nitrate (1 mL 0.2 M, 0.2 mmol) solution was increased up to 4.5 with 1.0 M aqueous piperazine hexahydrate in a 20 mL scintillation vial. A liquid-liquid solvent diffusion method with acetonitrile (1:2 solution:solvent) was implemented to aid in the crystallization of **U2-pip**.

$[(C_5H_6N)_2][(UO_2)_2(C_6H_5O_7)_2](H_2O)_4$: U2-py was synthesized with a 1:4 molar ratio of 0.2 M $UO_2(NO_3)_2{\cdot}6H_2O$ to 0.2 M $C_6H_8O_7{\cdot}H_2O$. The pH of a citric acid (4 mL 0.2 M, 0.8 mmol) and uranyl nitrate (1 mL 0.2 M, 0.2 mmol) solution was increased up to 4.5 with 50 v/v% aqueous pyridine in a 20 mL scintillation vial. A liquid-liquid solvent diffusion method with acetonitrile (1:2 solution:solvent) was implemented to aid in the crystallization of **U2-py**.

$[(C_2H_{10}N_2)][(UO_2)_2(C_6H_5O_7)_2](H_2O)_5$: U2-en was synthesized with a 1:4 molar ratio of 0.2 M $UO_2(NO_3)_2{\cdot}6H_2O$ to 0.2 M $C_6H_8O_7{\cdot}H_2O$. The pH of a citric acid (4 mL 0.2 M, 0.8 mmol) and uranyl nitrate (1 mL 0.2 M, 0.2 mmol) solution was increased up to 3.5 with 20 v/v% aqueous ethylenediamine in a 20 mL scintillation vial. A liquid-liquid solvent diffusion method with acetonitrile (1:2 solution:solvent) was implemented to aid in the crystallization of **U2-en**.

$[Na_4(C_4H_{12}N_2)_6][(UO_2)_6O_2(C_6H_4O_7)_6](H_2O)_{38}$: U3 was synthesized with a 1:2:1 molar ratio of 0.2 M $UO_2(NO_3)_2{\cdot}6H_2O$ to 0.2 M $C_6H_8O_7{\cdot}H_2O$ to 0.2 M NaOH. The pH of a citric acid (2 mL 0.2 M, 0.4 mmol), uranyl nitrate (1 mL 0.2 M, 0.2 mmol), sodium hydroxide (1 mL 0.2 M, 0.2 mmol) solution, with an additional 2 mL of water, was increased up to 6.5 with 1.0 M aqueous piperazine hexahydrate in a 20 mL scintillation vial and then potassium chloride (0.18 mL 0.2 M, 36 μmol) was incorporated into the reaction mixture to increase ionic strength. A liquid-liquid solvent diffusion method with tetrahydrofuran (1:1 solution:solvent) was implemented to aid in the crystallization of **U3**.

$[Na_9(Mg(H_2O)_4)_3][(UO_2)_9(OH)_3O_3(C_6H_4O_7)_6](H_2O)_{13}$: U9 was synthesized with a 1:2:1 molar ratio of 0.2 M $UO_2(NO_3)_2{\cdot}6H_2O$ to 0.2 M $C_6H_8O_7{\cdot}H_2O$ to 0.2 M NaOH. The pH of a citric acid (2 mL 0.2 M, 0.4 mmol), uranyl nitrate (1 mL 0.2 M, 0.2 mmol), sodium hydroxide (1 mL 0.2 M, 0.2 mmol) was increased up to 6.0 with 50 v/v% aqueous pyridine in a 20 mL scintillation vial and then magnesium nitrate (0.18 mL 0.2 M, 36 μmol) was incorporated into the reaction mixture to increase ionic strength. A liquid-liquid solvent diffusion method with tetrahydrofuran (1:1 solution:solvent) was implemented to aid in the crystallization of **U9**.

Single-Crystal X-ray Diffractometry. A suitable crystal of each compound and a small amount of the Paratone® N oil were collected on a MīTiGen cryoloop and transferred to a Nonius Kappa CCD single-crystal X-ray diffractometer equipped with graphite-monochromated Mo Kα radiation (λ = 0.7107 Å) and a low-temperature cryostat maintained at 100 K throughout the data collection. Nonius COLLECT software[1] was utilized for data acquisition and the intensity data were corrected for Lorentz, polarization, and background effects using the Bruker APEX II program.[2] A semi-empirical correction for crystal absorption was applied with the *SADABS* program.[2] All crystal structures were resolved by direct methods and refined on the basis of F^2 for all unique data using the Bruker SHELXTL version 5.01 software.[3] Selected data collection parameters and crystallographic information are provided in Table 2. **U2-pip** crystallized in a triclinic space group *P-1* with a = 6.7978(5) Å, b = 9.8815(8) Å, c = 11.7825(9) Å, α = 10.662(23) °, β = 99.5051(23) °, and γ = 91.0417(22) °. **U2-pry** crystallized in a triclinic space group *P-1* with a = 6.3074(4) Å, b = 10.0063(6) Å, c = 11.9920(7) Å, α = 94.6846(18) °, β = 98.8324(18) °, and γ = 104.5031(17) °. **U2-en** crystallized in a triclinic space group *P-1* with a = 6.2109(8) Å, b = 9.9970(13) Å, c = 11.3778(15) Å, α = 97.9088(37) °, β = 93.7875(37) °, and γ = 104.2937(36) °. **U3** crystallized in a triclinic space group *P-1* with a = 19.9870(8) Å, b = 20.5879(8) Å, c = 21.1208(8) Å, α = 68.4670(13) °, β = 64.4190(13) °, and γ = 67.9600(13) °. **U9** crystallized in a hexagonal group *P-63/m* with a = 17.4123(5) Å, b = 17.4123(5) Å, c = 17.8443(7) Å, α = 90°, β = 90°, and γ = 120°.

Direct methods were able to located the U and most of the Na, O, C, and N of the ligand and charge balancing cations. Unidentified atoms were then located in the difference Fourier maps. Hydrogen atoms bonded to carbon and nitrogen atoms were geometrically constrained using the appropriate AFIX commands. Hydrogen atoms bound to complexed and interstitial water molecules for **U2-pip**, **U2-pry**, and **U2-en** were determined in the difference Fourier maps and appropriate DFIX restraints were applied to create a reasonable H-bonding network. For the data analysis of **U9**, highly disordered regions of the interstitial space between the molecular clusters were modeled as a diffuse contribution using the SQUEEZE algorithm supplied in the PLATON program[4,5]. It was determined that there were two regions within the unit cell at (0.333 0.667 0.750) and (0.667 0.333 0.250) that contained 8 sodium cations and 24 water molecules distributed between the two locations. Further details the structure determination for each compound can be found in their respective CIF files.

Table S1. Selected crystallographic information for $[C_4H_{12}N_2][(UO_2)_2(C_6H_5O_7)_2](H_2O)_6$ (**U2-pip**), $[(C_5H_6N)_2][(UO_2)_2(C_6H_5O_7)_2](H_2O)_4$ (**U2-py**), $[(C_2H_{10}N_2)][(UO_2)_2(C_6H_5O_7)_2](H_2O)_5$ (**U2-en**), $[Na_4(C_4H_{12}N_2)_6][(UO_2)_6O_2(C_6H_4O_7)_6](H_2O)_{38}$ (**U3**), and $[Na_9(Mg(H_2O)_4)_3][(UO_2)_9(OH)_3O_3(C_6H_4O_7)_6](H_2O)_{13}$ (**U9**).

	U2-pip	**U2-py**	**U2-en**	**U3**	**U9**
FW (g mol^{-1})	1150.54	1114.51	1070.46	4009.62	4396.63
Space group	*P-1*	*P-1*	*P-1*	*P-1*	*P-63/m*
a **(Å)**	6.7978(5)	6.3074(4)	6.2109(8)	19.9870(8)	17.4123(5)
b **(Å)**	9.8815(8)	10.0063(6)	9.9970(13)	20.5879(8)	17.4123(5)
c **(Å)**	11.7825(9)	11.9920(7)	11.3778(15)	21.1208(8)	17.8443(7)
α **(°)**	100.662(23)	94.6846(18)	97.9088(37)	68.4670(13)	90
β **(°)**	99.5051(23)	98.8324(18)	93.7875(37)	64.4190(13)	90
γ **(°)**	91.0417(22)	104.5031(17)	104.2937(36)	67.9600(13)	120
V **(Å^3)**	766.15(10)	718.32(8)	674.38(15)	7044.4(5)	4685.4(3)
Z	1	1	1	2	2
ρ_{calc} (mg m^{-3})	2.494	2.576	2.636	1.890	2.896
μ (mm^{-1})	10.654	11.363	12.095	6.993	15.659
F (000)	536	520	496	3776	3620
Crystal Size (mm)	0.180 x 0.080 x 0.080	0.200 x 0.200 x 0.060	0.220 x 0.045 x 0.020	0.280 x 0.180 x 0.140	0.120 x 0.120 x 0.080
Theta Range (°)	2.480 to 27.410	2.560 to 27.450	2.570 to 30.420	1.169 to 29.575	2.280 to 26.690
Data Collected	-8 < h < 8 -12 < k < 12 -15 < l < 15	-7 < h < 8 -12 < k < 12 -15 < l < 15	-7 < h < 8 -13 < k < 13 -14 < l < 14	-27 < h < 27 -28 < k < 25 -29 < l < 29	-21 < h < 21 -21 < k < 21 -22 < l < 22
Reflections Collected/ Unique	19 074/3482 [R_{int} = 0.0263]	14 292/3280 [R_{int} = 0.0304]	16 340/3222 [R_{int} = 0.0259]	169 551/39500 [R_{int} = 0.0224]	95 326/3421 [R_{int} = 0.0351]
GOF of F^2	1.077	1.081	1.098	1.048	1.001
Final *R* Indices [I > 2σ(I)]	R_1 = 0.0134 wR_2 = 0.0321	R_1 = 0.0259 wR_2 = 0.0626	R_1 = 0.0217 wR_2 = 0.0555	R_1 = 0.0365 wR_2 = 0.1013	R_1 = 0.0299 wR_2 = 0.0774
R **Indices (all data)**	R_1 = 0.0150 wR_2 = 0.0327	R_1 = 0.0269 wR_2 = 0.0632	R_1 = 0.0230 wR_2 = 0.0561	R_1 = 0.0451 wR_2 = 0.1070	R_1 = 0.0368 wR_2 = 0.0834

Table S2. Average bond lengths and bond angles associated with the citrate compounds.

Average Bond Lengths	**U2-pip**	**U2-py**	**U2-en**	**U3**	**U9**
Single-Crystal X-ray Diffraction					
U-O_{ax} Bond Distance (Å)	1.779(4)	1.774(18)	1.777(3)	1.798(3)	1.801(6)
U-O_{eq} Bond Distances (Å)	2.374(4)	2.384(16)	2.374(3)	2.348(3)	2.327(5)
U···U Distance (Å)	3.890	3.908	3.907	3.758	3.798
μ_2-(O···O) Distance (Å)	2.711	2.710	2.705	2.591	2.534
μ_3-(O-U) Distance (Å)	-	-	-	2.241	2.193
Na···O Distance (Å)	-	-	-	2.352	2.426

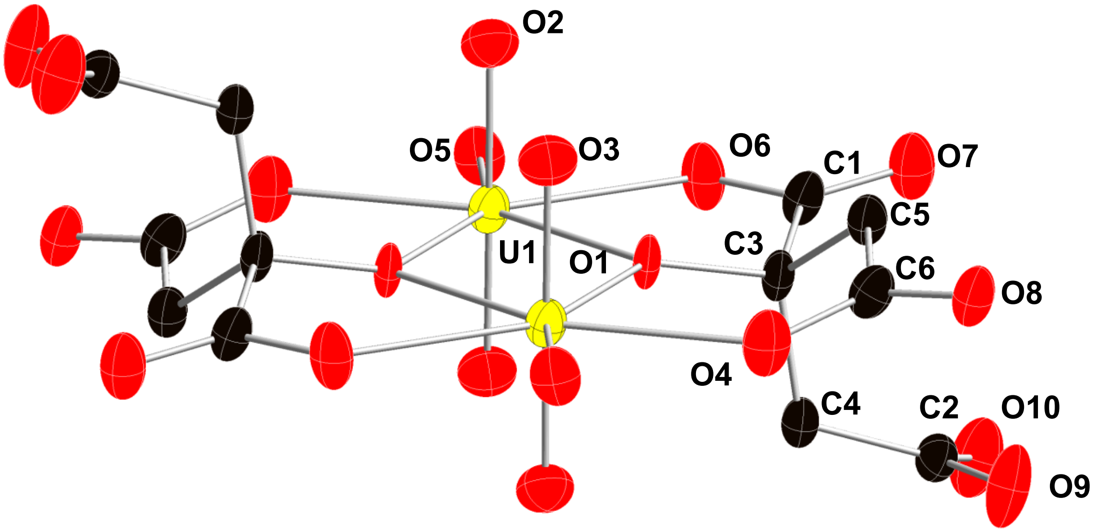

Figure S1. The (**U2**) 2:2 U:*Cit* species is shown as a thermal ellipsoid representation (50%). Hydrogen atoms were omitted for clarity.

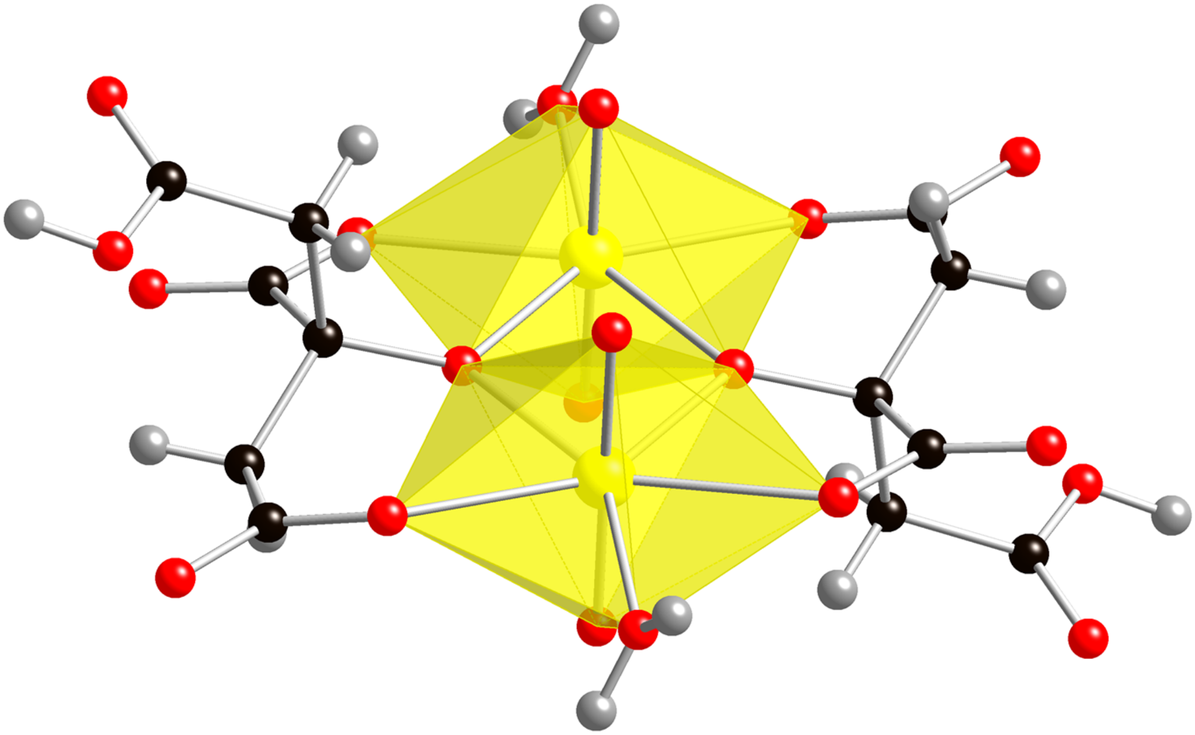

Figure S2. Ball and stick model of the U2 molecule including the H atom. The orientation is identical to that shown in figure S1 to provide information on atom labels. The U is represented by translucent yellow polyhedra and the C, O, and H atoms are depicted as black, red, and grey spheres, respectively.

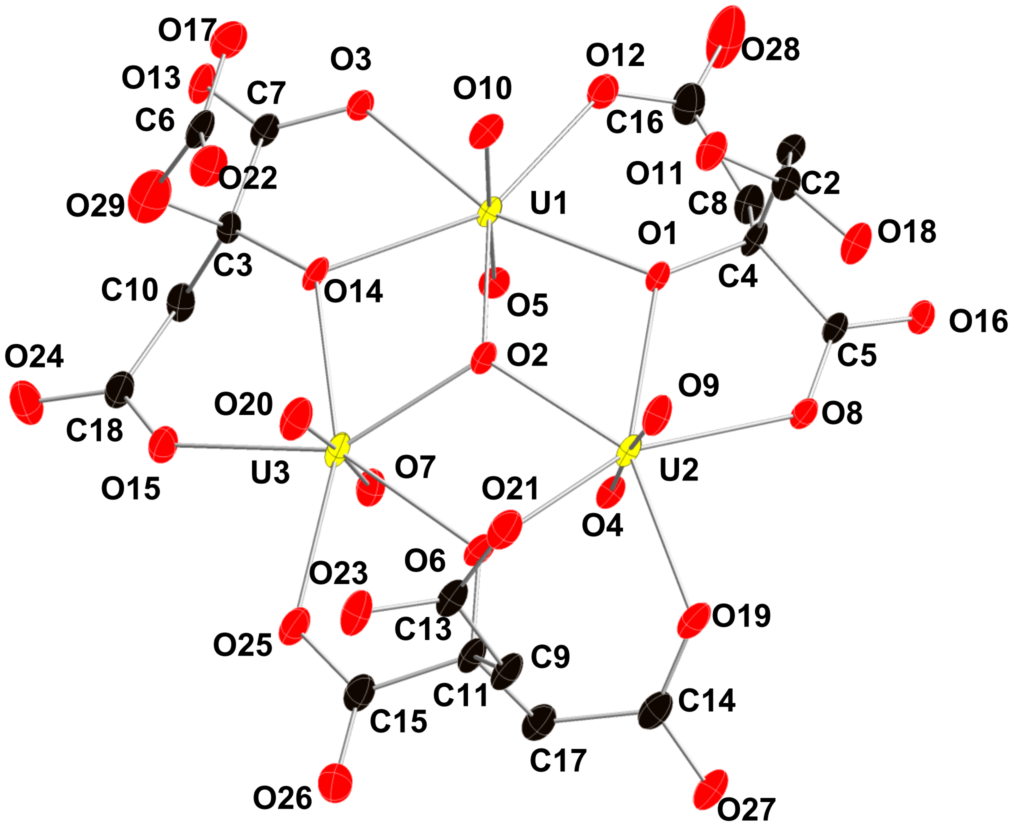

Figure S3. Two crystallographically unique trimers are present in **U3**, with the first shown with thermal ellipsoids (50%). Hydrogen atoms were omitted for clarity.

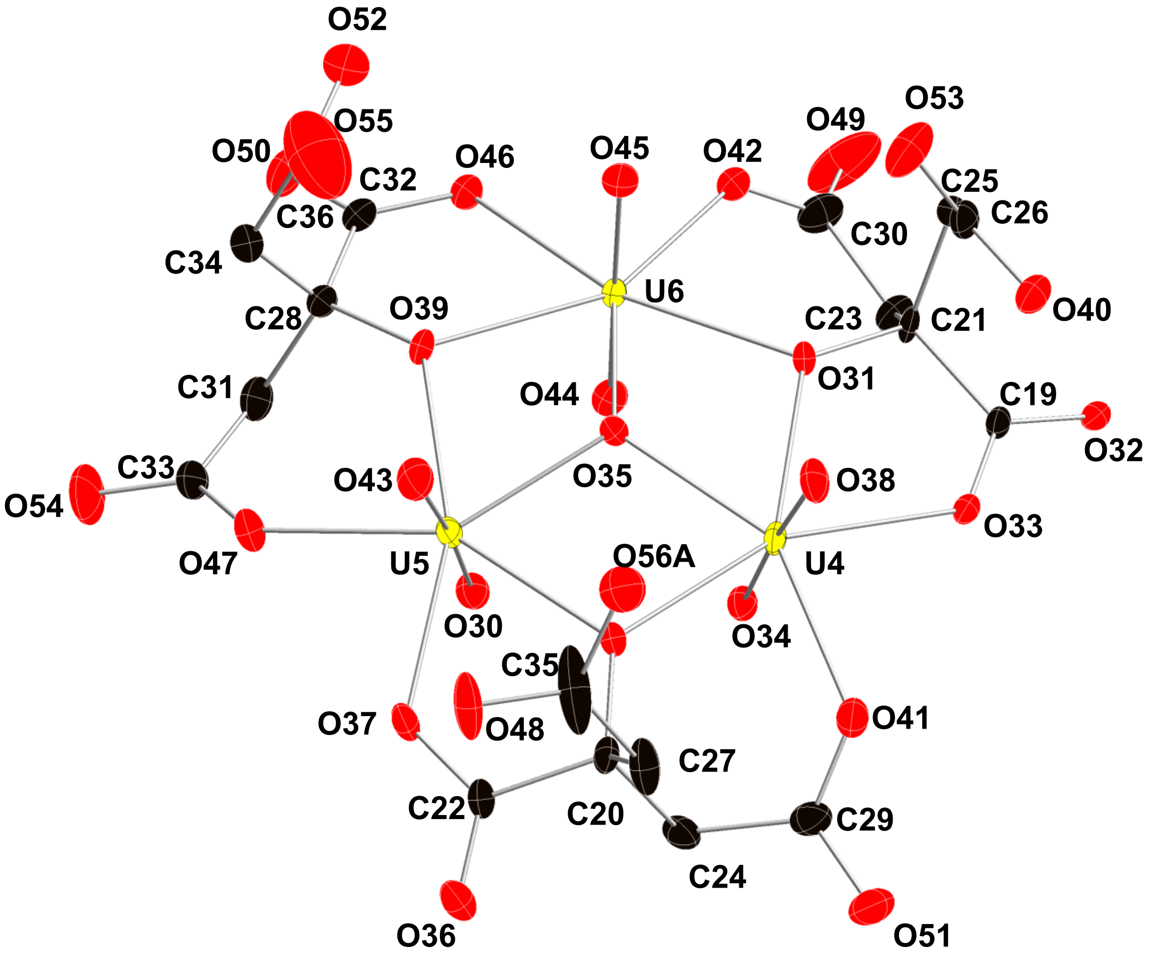

Figure S4. The 3:3 species (**U3**) has two crystallographic unique trimeric species and the second cluster is shown above with a thermal ellipsoid model (50%). Hydrogen atoms were omitted for clarity.

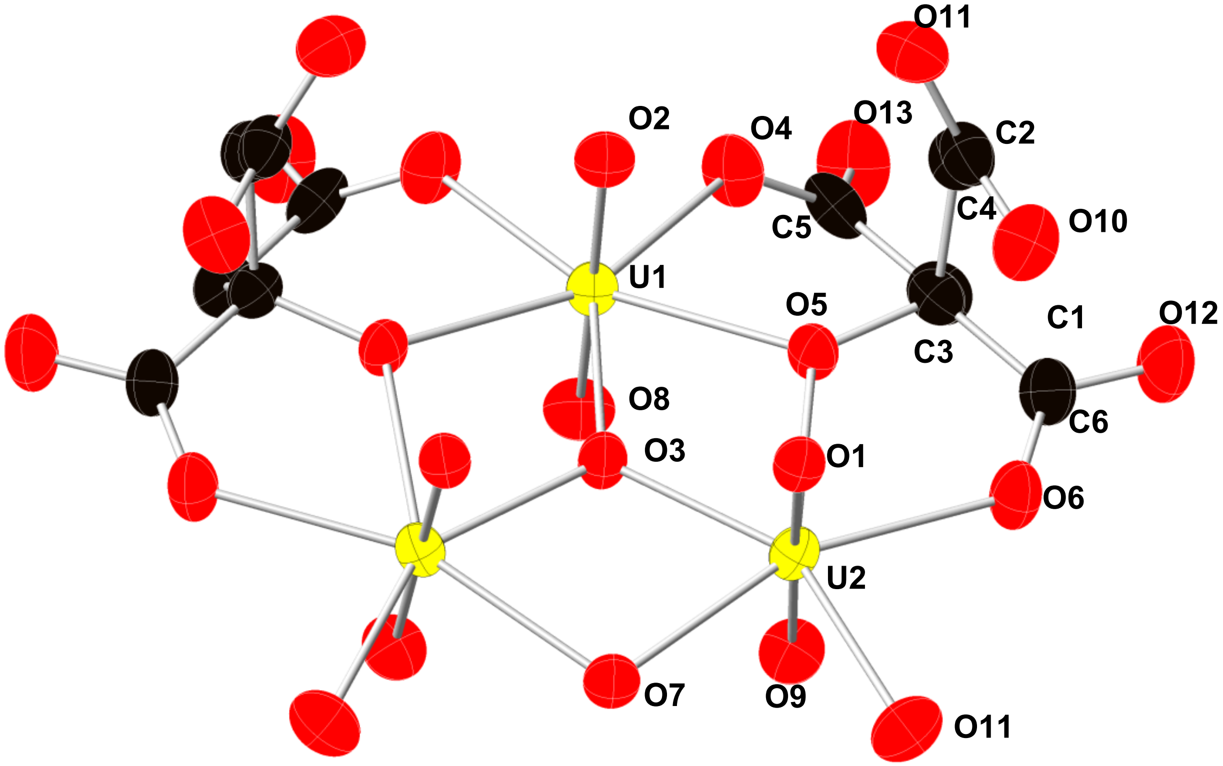

Figure S5. Thermal ellipsoid model (50%) of the 3:2 subunit that is present in the **U9** 9:6 macrocycle. Hydrogen atoms were omitted for clarity.

Powder X-ray Diffractometry. A Bruker D-5000 Advanced Powder Diffractometer equipped with Cu Kα radiation (λ = 1.5418 Å) and a LynxEye position sensitive detector was utilized to confirm the purity of each compound before further characterization. The diffractogram scans were preformed from 5-60° 2*Θ* with a step size of 0.02° 2*Θ* and a count time of 0.5 sec/step and then compared to calculated patterns using the Mercury 3.3 software.

Thermogravimetric analysis on crystalline material.

The hydration state of the **U2, U3, and U9** compounds were analyzed with a TA Instruments TGA Q500 to quantify the total water content and hydration states. An aluminum pan was loaded with approximately 10-15 mg of each sample and heated in air at a ramp rate of 2 °C/min from 25 – 600 °C.

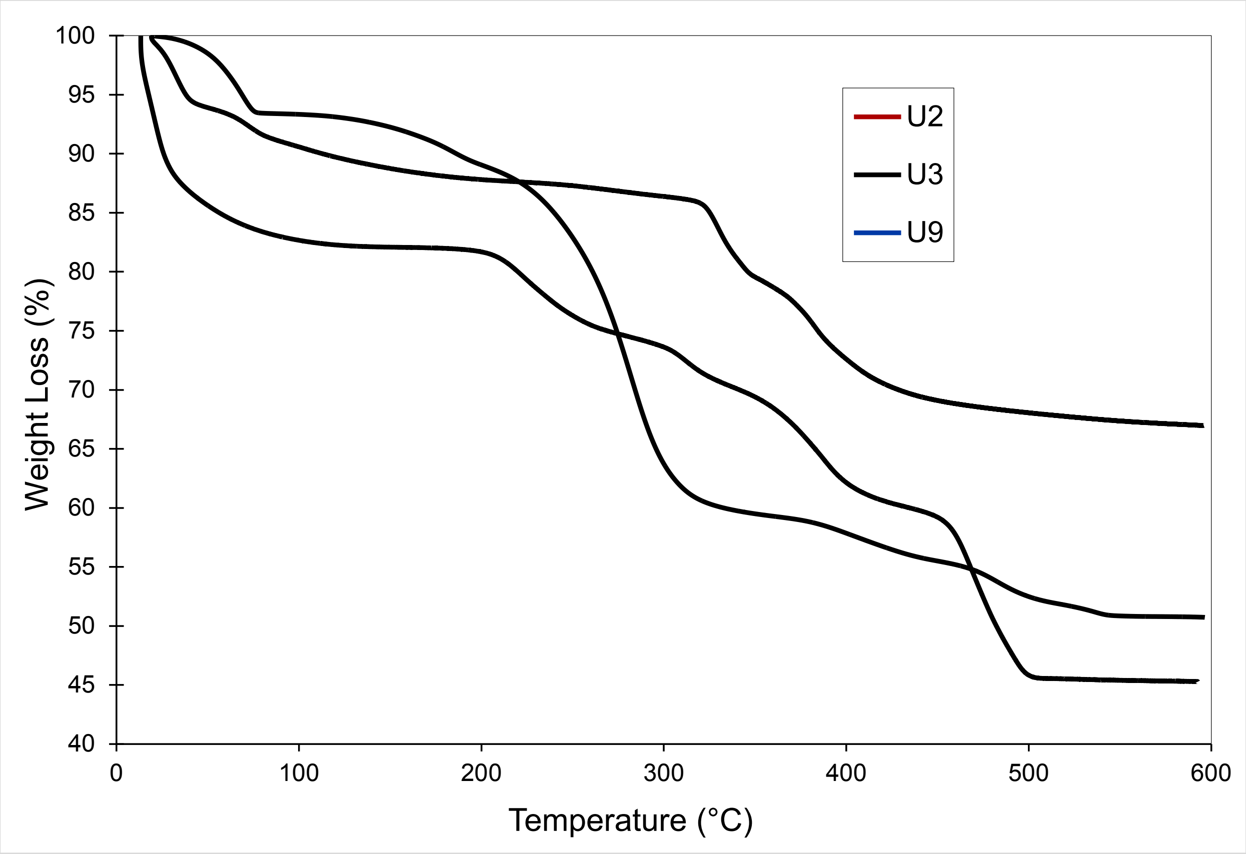

Figure S6. Thermogravimetric analysis of the crystalline **U2**, **U3**, and **U9** compounds.

Vibrational Spectroscopy on solid state materials. In order to investigate citrate chelation and water solvation, the bending and stretching vibrational modes of **U2**, **U3**, and **U9** were evaluated with Fourier Transform Infrared Spectroscopy and High Resolution Raman Spectroscopy. Infrared spectra of each compound, with KBr as the binding agent, were collected from 500-4000 cm^{-1} on a Nicolet FTIR Spectrometer. Raman spectra of a single crystal from each compound were collected on a Nicolet Almega XR High Performance Dispersive Spectrometer with a 785 nm excitation laser.

Fourier Transform infrared spectroscopy validates that the citrate ligands chelate to the uranium metal center and that solvated water groups are present. The characteristic asymmetric stretching vibration of the uranyl cation is observed in **U2**, **U3**, and **U9** at 917 cm^{-1}, 890 cm^{-1}, and 880 cm^{-1}, respectively (Figure S7). All three compounds display both the symmetric, 1385-1395 cm^{-1}, and asymmetric, 1550-1590 cm^{-1}, stretching vibrations for the deprotonated $–COO^-$ functional groups on the citric acid chelator. In the spectra associated with the **U3** and **U9** compounds, an absence of the protonated –COOH vibrational mode at approximately 1710 cm^{-1} indicates that all of the carboxyl groups on the citric acid ligand are deprotonated. However, the protonated carboxylate frequency is observed for the **U2** compound at 1725 cm^{-1} due to the fact that the citrate ligand chelates **U2** in a tridendate manner which leaves one carboxyl group protonated. A broad frequency band is present for all three compounds from 2500-3600 cm^{-1} as a result of O-H stretching vibrations from ligated water molecules and the bridging hydroxyl groups. Two noticeable frequencies on the **U3** spectrum at 3000 cm^{-1} and 3250 cm^{-1} correspond to the vibrational frequencies of C-H and N-H stretching, respectively, arising from the large amount of solvated piperazinium groups in that compound.

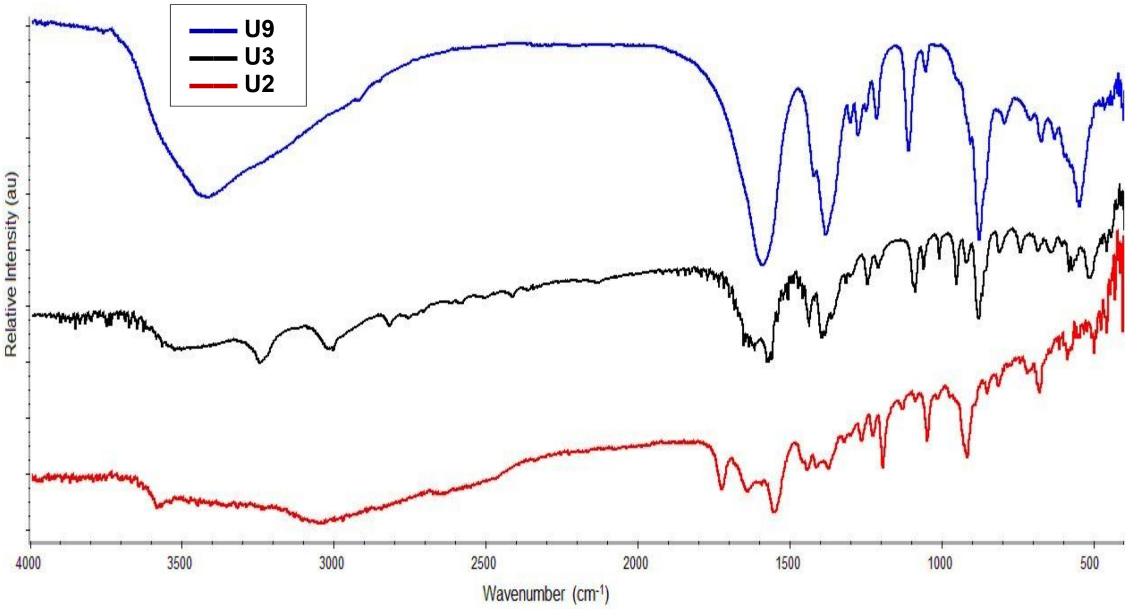

Figure S7. The infrared spectra for **U2**, **U3**, and **U9** validate the citric acid tridentate chelation on the uranyl metal center and confirm the presence of solvated water molecules in the crystalline material.

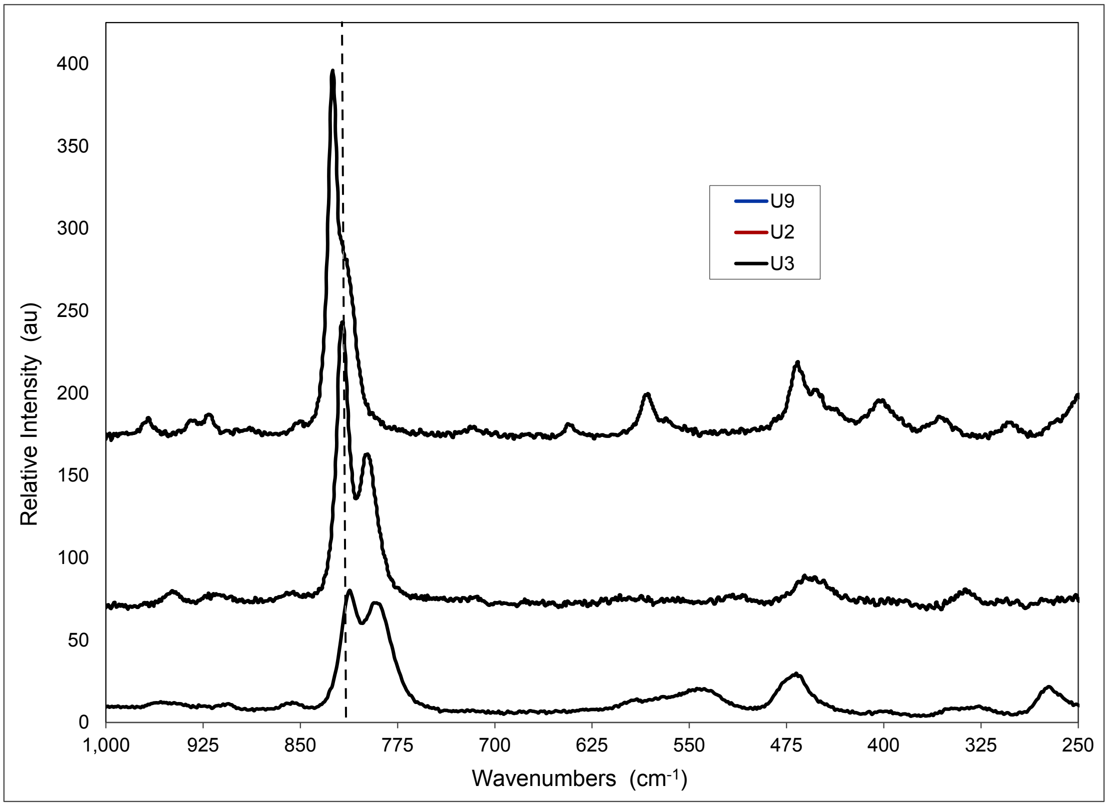

Figure S8. The Raman spectra for **U2**, **U3**, and **U9** demonstrate the intense ν_1 symmetric stretching vibration observed for the UO_2^{2+} cation. The red shifted frequency bands explain the solvation of the uranyl cation by the electron donating functional groups on citric acid. An additional band associated with the citrate molecule is located at 812 cm^{-1}.

Solution Raman Spectra studies.

Under aqueous conditions, pH variations greatly affects oligomerization and the lability of the citrate ligand. Complementary analysis, using Raman spectroscopy, was implemented to better understand uranium-citrate aggregation in the **U2**, **U3**, and **U9** pre-crystallization solution. To comprehensively interpret the pH-dependency of uranium-citrate oligomers, a 1:1 (50 mM U:50 mM Cit) and a 1:2 (50 mM U:100 mM Cit) concentration ratio were examined each at pH values of 3.00, 5.00, 7.00, and 9.00. The pH of each sample was adjusted with 1.0 M HNO_3 and 1.0 M NaOH and allowed at least 30 minutes to equilibrate before data acquisition. The analysis was conducted on a high-resolution B&W Tek i-Raman Spectrometer equipped with a 785 nm excitation laser and a 2048 pixel CCD transducer. The output power from the 785 nm laser source was set to 81.0 mW and each acquired spectrum was averaged 15 times with a 20 second integration time.

In order to conclusively understand the aggregate speciation, peak fitting was utilized to define and resolve the previously mentioned signals. OriginPro 9.1.0 64-bit software refined the spectra, fit each of the peaks with a Gaussian function and all the fitting parameters converged with a chi-squared tolerance value of 10^{-14}. The results are summarized in Table S3. The nitrate signal at 1048 cm^{-1} was included in the peak fitting analysis as an internal reference to make relative correlations between the signals of interest. For both pH 3.00 and pH 5.00, OriginPro could not fit a peak to the 814 cm^{-1} citrate peak due to the overlap from the large **U2** dimer signal. At pH 3.00, the dominate signal is observed at 826 cm^{-1} and is approximately 4.5 times larger than the minor peak in both the 1:1 and 1:2 samples. At pH 5.00, again the dominate signal is seen at 826 cm^{-1} but the signal intensity is about 2.5 times larger than the minor peak due to a decrease in the 826 cm^{-1} signal intensity and an increase in signal intensity from the minor peak. For both pH 7.00 and pH 9.00, OriginPro successfully fit the 814 cm^{-1} citrate peak. In the 1:1 trials, the dominate peak was fit to 793 cm^{-1}, the $[(UO_2)_3(Cit)_2]^{2-}$ aggregate, for both pH 7.00 and pH 9.00. In the 1:2 trials, the dominate peak was fit to 797 cm^{-1}, the $[(UO_2)_3(Cit)_3]^{6-}$ aggregate, for both pH 7.00 and pH 9.00.

Table S3. Data processing of the Raman spectra obtained from aqueous solutions containing 1:1 or 1:2 U:cit.

	50 mM Uranium, 50 mM Citrate			*50 mM Uranium, 100 mM Citrate*		
	pH 3.00			**pH 3.00**		
Raman Signal (cm^{-1})	1048	827	792	1048	827	797
Signal Height ($Cts \cdot mW^{-1} \cdot s^{-1}$)	0.269	0.281	0.060	0.337	0.351	0.080
Normalized Height Relative to 1048 cm^{-1}	1.000	1.043	0.223	1.000	1.042	0.238
	pH 5.00			**pH 5.00**		
Raman Signal (cm^{-1})	1048	826	793	1048	826	797
Signal Height ($Cts \cdot mW^{-1} \cdot s^{-1}$)	0.251	0.211	0.085	0.298	0.240	0.096
Normalized Height Relative to 1048 cm^{-1}	1.000	0.840	0.337	1.000	0.803	0.323
	pH 7.00			**pH 7.00**		
Raman Signal (cm^{-1})	1048	814	793	1048	814	796
Signal Height ($Cts \cdot mW^{-1} \cdot s^{-1}$)	0.247	0.121	0.187	0.301	0.091	0.209
Normalized Height Relative to 1048 cm^{-1}	1.000	0.491	0.757	1.000	0.303	0.692
	pH 9.00			**pH 9.00**		
Raman Signal (cm^{-1})	1048	814	793	1048	814	797
Signal Height ($Cts \cdot mW^{-1} \cdot s^{-1}$)	0.300	0.129	0.201	0.315	0.074	0.247
Normalized Height Relative to 1048 cm^{-1}	1.000	0.432	0.671	1.000	0.235	0.784

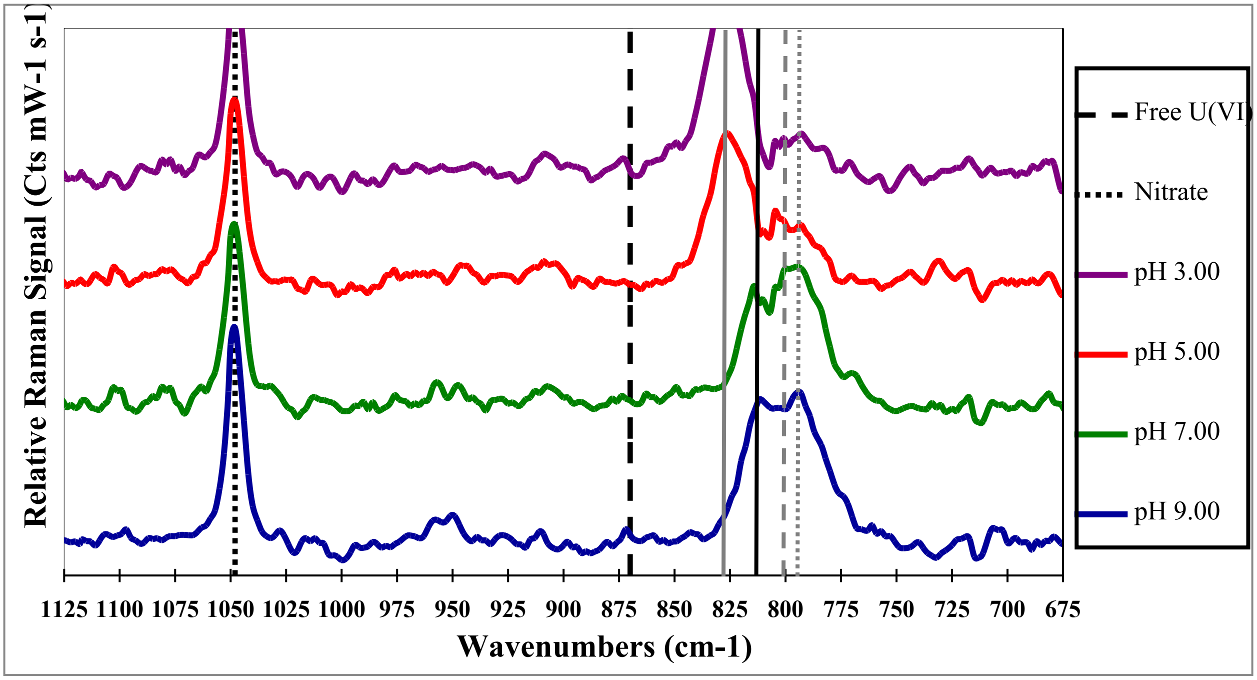

Figure S9. Raman spectra of the 1:1 uranyl citrate solution at varying pH values with a dotted line for the free nitrate (1047 cm^{-1}), dashed line for the predicted free uranyl (870 cm^{-1}) and a solid black line corresponds to the citrate peak (812 cm^{-1}). The uranyl citrate species are observed at 826 cm^{-1} (solid grey line), 797 cm^{-1} (dashed grey line), and 792 cm^{-1} (dotted grey line).

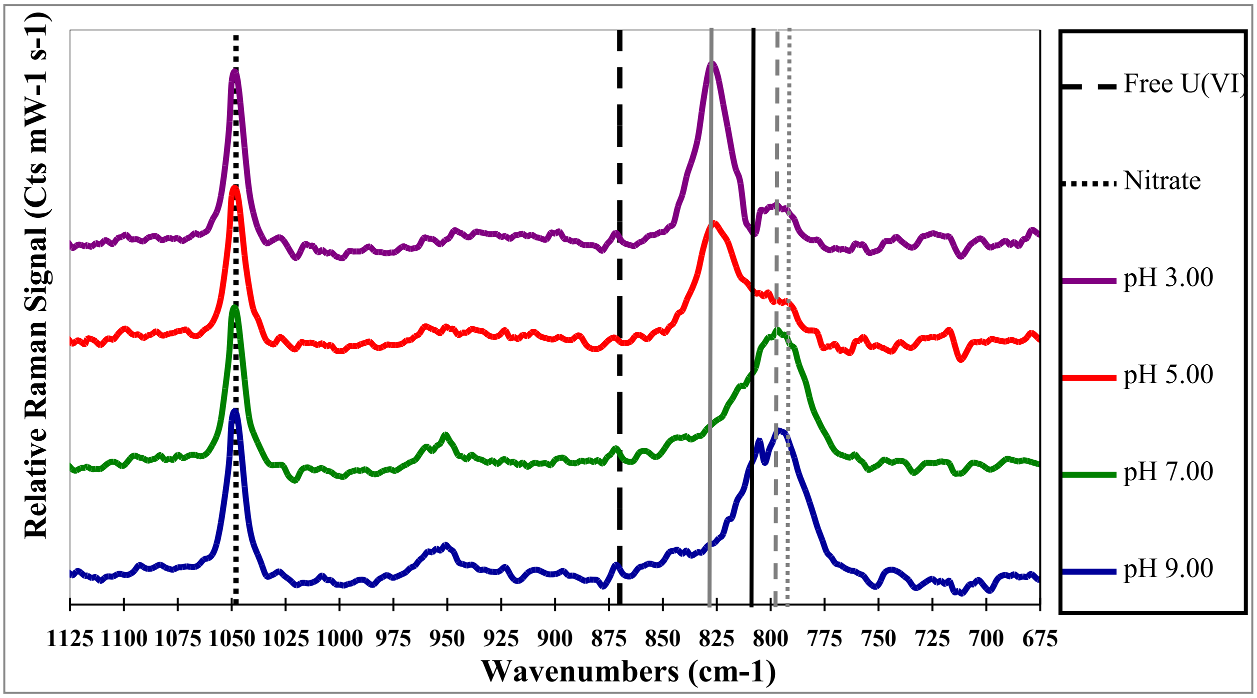

Figure S10. Raman spectra of the 1:2 (uranyl:citrate) solution (pH 3-9). Lines on the spectra correspond to free nitrate (dotted black line, 1047 cm^{-1}), uranyl (dashed black line, 870 cm^{-1}) and the citrate peak (solid black line, 812 cm^{-1}). The uranyl citrate species are observed at 826 cm^{-1} (solid grey line), 797 cm^{-1} (dashed grey line), and 792 cm^{-1} (dotted grey line).

sMass Spectroscopy.

The presence of stabilized aggregates of **U2**, **U3**, and **U9** were examined by electrospray ionization mass spectrometry (ESI-MS), as anions in an aqueous matrix. Mass spectra were collected on a ThermoElectron LCQ Deca Quadrupole Ion-Trap Mass Spectrometer operated in negative ion mode. Electrospray conditions were maintained throughout the experiment. Samples were flowed via direct infusion with a 250 μL Hamiltonian glass syringe at a flow rate of 20 μL min^{-1} using nitrogen as the nebulizing gas. The capillary temperature within the ESI source was set at 110 °C to promote effective dissolution and a capillary voltage of -16 kV was used throughout the experimental trials. Additional programmable ESI parameters were set as follows: ionization spray voltage, 3.5 kV; tube lens offset voltage, 20 V. Fragmentation of the molecular species present in the solid state compounds were investigated by dissolving a small amount of the crystallites in aqueous solutions where the pH was varied between 6.5 and 10.0 by addition of 1M ammonium hydroxide buffer. In all solutions, the fragmentation pattern was identical. Solutions with U:Cit ratios of 1:1 (50 mM U:50mM Cit) and 1:2 (50mM U:100mM Cit) concentration ratio were prepared at pH values of 3.00, 5.00, 7.00, and 9.00 using NH_4OH as a buffer. The resulting data is summarized in Table S4.

Table S4. ESI-MS assignments of the 1:1 and 1:2 U:Cit solutions for major species.

pH	1:1 U:Cit **(m/z, relative %, species)**	1:2 U:Cit **(m/z, relative %, species)**
3	m/z = 456, 100% $[UO_2\text{-}2OH\text{-}3H\mathit{Cit} + 5H^+ + 2NH_4^+]^{2-}$	m/z = 456, 100% $[UO_2\text{-}2OH\text{-}3H\mathit{Cit} + 5H^+ + 2NH_4^+]^{2-}$
5	m/z = 456, 100% $[UO_2\text{-}2OH\text{-}3H\mathit{Cit} + 5H^+ + 2NH_4^+]^{2-}$	m/z = 476, 100% $[3UO_2\text{-}O\text{-}3H\mathit{Cit} + 2NH_4^+]^{3-}$ m/z = 471, 88% $[3UO_2\text{-}2OH\text{-}3H\mathit{Cit} + 2H^+]^{3-}$ m/z = 486.5, 60% $[2UO_2\text{-}OH\text{-}2O\text{-}2H\mathit{Cit} + 5H^+]^{2-}$ m/z = 401.6, 58% $[3UO_2\text{-}2O\text{-}H\mathit{Cit} + 4\ NH_4^+]^{3-}$ m/z = 571.5, 49% $[2UO_2\text{-}2OH\text{-}3H\mathit{Cit} + 2H^+ + NH_4^+]^{2-}$ m/z = 456, 100% $[UO_2\text{-}2OH\text{-}3H\mathit{Cit} + 5H^+ + 2NH_4^+]^{2-}$
7	m/z = 456, 100% $[UO_2\text{-}2OH\text{-}3H\mathit{Cit} + 5H^+ + 2NH_4^+]^{2-}$ m/z = 471, 62% $[3UO_2\text{-}2OH\text{-}3H\mathit{Cit} + 2H^+]^{3-}$ m/z = 476, 31% $[3UO_2\text{-}O\text{-}3H\mathit{Cit} + 2NH_4^+]^{3-}$	m/z = 476, 100% $[3UO_2\text{-}O\text{-}3H\mathit{Cit} + 2NH_4^+]^{3-}$ m/z = 471, 89% $[3UO_2\text{-}2OH\text{-}3H\mathit{Cit} + 2H^+]^{3-}$ m/z = 486.5, 80% $[2UO_2\text{-}OH\text{-}2O\text{-}2H\mathit{Cit} + 5H^+]^{2-}$ m/z = 456, 73% $[UO_2\text{-}2OH\text{-}3H\mathit{Cit} + 5H^+ + 2NH_4^+]^{2-}$ m/z = 401.6, 70% $[3UO_2\text{-}2O\text{-}H\mathit{Cit} + 4\ NH_4^+]^{3-}$ m/z = 571.5, 52% $[2UO_2\text{-}2OH\text{-}3H\mathit{Cit} + 2H^+ + NH_4^+]^{2-}$
9	m/z = 456, 100% $[UO_2\text{-}2OH\text{-}3H\mathit{Cit} + 5H^+ + 2NH_4^+]^{2-}$ m/z = 426, 88% $[2UO_2\text{-}2OH\text{-}2O\text{-}H\mathit{Cit} + 3\ NH_4^+]^{2-}$ m/z = 486.5, 57% $[2UO_2\text{-}OH\text{-}2O\text{-}2H\mathit{Cit} + 5H^+]^{2-}$ m/z = 401.6, 55% $[3UO_2\text{-}2O\text{-}H\mathit{Cit} + 4\ NH_4^+]^{3-}$ m/z = 571.5, 52% $[2UO_2\text{-}2OH\text{-}3H\mathit{Cit} + 2H^+ + NH_4^+]^{2-}$	m/z = 394, 100% $[2UO_2\text{-}2OH\text{-}2O\text{-}3H\mathit{Cit} + 8\ H^+\ ]^{3-}$ m/z = 406, 38% $[3UO_2\text{-}2O\text{-}2H\mathit{Cit} + H^+]^{3-}$ m/z = 432, 34% $[3UO_2\text{-}3OH\text{-}2O\text{-}2H\mathit{Cit} + 6\ H^+ + NH_4^+]^{3-}$

Dynamic Light Scattering Experiments

A solution containing the U:Cit ratio of approximately 1:2 was buffered to a pH of 6 using 1 M NaOH was placed in a plastic cuvette with a snap-top lid. The sample was placed on a Malvern Dynamic Light Scattering instrument equipped with a He-Ne laser (λ = 633 nm) and a backscatter detector (Fig. S11).

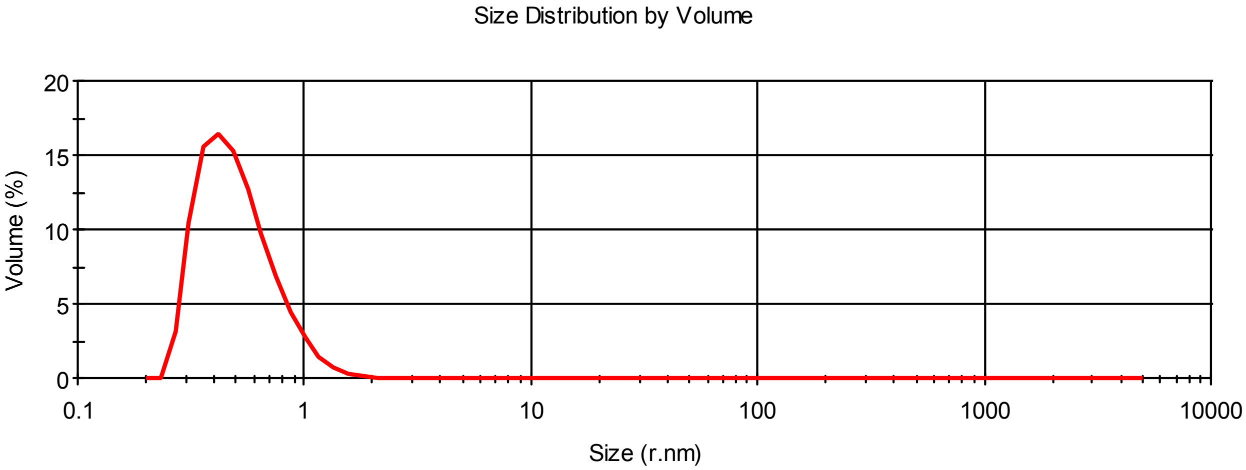

Figure S11. Size distribution obtained from the solution that contained U:*Cit* in a 1:2 ratio, indicating the presence of a larger self-assembled molecules.

References

1. R. W. W. Hoft, *COLLECT*, (1998), Delft, The Netherlands.
2. G. M. Sheldrick, *APEX II*, (1996) Bruker AXS, Madison, WI.
3. G. M. Sheldrick, *Acta Crystallographica Section A: Foundations of Crystallography*, 2008, **64**, 112-122.
4. P. Vandersluis; A. L. Spek, *Acta Crystallographica Section A*, 1990, **46**, 194-201.
5. A. L. Spek, *Applied Crystallography*, 2003, **36**, 7-13.